ELSEVIER

Journal of Molecular Catalysis A: Chemical 165 (2001) 249–263

JOURNAL OF MOLECULAR CATALYSIS A: CHEMICAL

www.elsevier.com/locate/molcata

A transient FTIR study of species formed during NO_x storage in the $Pt/BaO/Al_2O_3$ system

Björn Westerberg [a,b], Erik Fridell [b,c,*]

[a] Department of Chemical Reaction Engineering, Chalmers University of Technology, SE-412 96 Göteborg, Sweden
[b] Competence Centre for Catalysis, Chalmers University of Technology, SE-412 96 Göteborg, Sweden
[c] Department of Applied Physics, Chalmers University of Technology and Göteborg University, SE-412 96 Göteborg, Sweden

Received 24 May 2000; accepted 11 September 2000

Abstract

FTIR spectroscopy has been used to study samples of Al_2O_3, Pt/Al_2O_3, BaO/Al_2O_3 and $Pt/BaO/Al_2O_3$ under exposure to either NO_2 and O_2 or NO and O_2, between 100 and 400°C. The resulting spectra are fitted to various species, mainly nitrites and nitrates, formed on Al_2O_3 and BaO. The exposure of NO_2 and O_2 on the Al_2O_3 sample results in the formation of monodentate, bridged and bidentate nitrates. The relative abundance of these nitrate species change with temperature. The obtained enthalpy changes for transition from monodentate to bridged nitrate and from monodentate to bidentate nitrate are -7.7 and 7.4 kJ/mol, respectively. The corresponding entropy changes are -7.1 and 30.2 J/mol K, respectively. For NO and O_2, lower concentrations of nitrates are detected as well as both linear and bridged nitrites. When Pt is present in the catalyst, NO is oxidised to NO_2 at temperatures above 150°C resulting in the formation of large amounts of nitrates. It seems as if the formation of nitrites proceed the formation of nitrates. For the samples with both BaO and Al_2O_3, similar species as outlined above are observed on Al_2O_3 while mainly nitrites and hyponitrites are observed on Ba when exposed to $NO + O_2$ below 200°C. When exposed to $NO_2 + O_2$, nitrates are formed on BaO as well as two features attributed to bidentate and bridged nitrate on alumina at the alumina–barium oxide interface. Formation of bulk $Ba(NO_3)_2$ was not observed. It is concluded that Al_2O_3 plays an important role as a storage site at $100°C \leq T \leq 300°C$ and by providing a large surface area for BaO. There are also indications that nitrates formed on Al_2O_3 may spill over to BaO.

Keywords: FTIR spectroscopy; $Pt/BaO/Al_2O_3$ system; NO_x reduction; NO_x storage; Surface nitrates; Surface nitrites

---

1. Introduction

The need to decrease the emissions of fossil CO_2 into the atmosphere will put pressure on car manufacturers to improve the fuel efficiency of their products. One contribution to this can be to replace the stoichiometric gasoline engines with lean-burn engines [1]. However, this leads to the problem of reducing nitrogen oxides in the exhaust under lean conditions over a wide temperature range. This cannot be achieved with the common three-way catalyst.

One possible concept for reduction of NO_x under lean-burn conditions is to use so called NO_x storage catalysts in combination with mixed lean operation of the engine [2–4]. In this case, NO_x is stored in the catalyst under lean conditions and the catalyst is regenerated during short periods of rich conditions. During the latter, the stored NO_x is released and reduced to N_2.

Model NO_x storage catalysts have been examined by IR in few cases [2,4–6]. Takahashi et al. [2] reported

---

[*] Corresponding author. Tel.: +46-31-772-2961; fax: 46-31-772-2967.
E-mail address: fridell@fy.chalmers.se (E. Fridell).

PII: S1381-1169(00)00431-3

a peak at 1350 cm^{-1} attributed to NO_3 anions. Coronado and Anderson [6] studied NO_2 adsorption on a $Pt/BaCl_2/SiO_2$ sample and assign major peaks at 1418 and1360 cm^{-1} to the formation of $Ba(NO_3)_2$. They also claim to observe the formation of $ClNO_2$ and NO adsorbed on Pt. Fridell et al. [4,5] observed nitrates and carbonates in lean mixtures of NO, O_2 and C_3H_6 over a $Pt/BaO/Al_2O_3$ catalyst. They measured at various temperatures and found the largest amount of nitrates close to 370°C. When switching to a rich mixture of NO and C_3H_6 an isocyanate peak becomes apparent.

A slightly different approach is to try to selectively reduce nitrogen oxides by a specific reductant, added to the exhaust. This reducing agent should preferably be the fuel used in the vehicle. Although this concept has been studied intensively, the NO_x reduction efficiency is not yet satisfactory [7]. From FTIR studies, isocyanate and organic nitro species have been found during reaction for Pt/SiO_2 [8], isocyanate and cyanide on Pt/Al_2O_3 [9–11].

The purpose of this work is to systematically study the interaction of NO or NO_2 and O_2 with model NO_x storage and reduction catalysts ($Pt/BaO/Al_2O_3$). In order to examine the influence of the different components, four different samples, $Pt/BaO/Al_2O_3$, Pt/Al_2O_3, BaO/Al_2O_3, and Al_2O_3 are investigated in situ by transmission FTIR at different times of exposure and different temperatures. This yields information on which compounds that are present as well as the storage dynamics. IR studies are very well suited for this type of investigations where the dynamics of a stored compound is to be studied. For studies of reaction intermediates, on the other hand, these are often present in low concentrations while by-products on the support give large IR features.

2. Experimental methods

2.1. Catalyst preparation

Four different catalysts were prepared as described in [4]: γ-Al_2O_3, Pt/γ-Al_2O_3, BaO/γ-Al_2O_3 and $Pt/BaO/\gamma$-Al_2O_3. The Ba content in the BaO/Al_2O_3 and $Pt/BaO/Al_2O_3$ catalysts was 20% BaO by weight, and the platinum content in the Pt/Al_2O_3 and $Pt/BaO/Al_2O_3$ catalysts was 2% Pt by weight. γ-Al_2O_3 was prepared by calcining boehmite (Disperal, Condea) powder at 600°C for 8 h. The BaO/Al_2O_3 catalyst was prepared by dissolving barium nitrate in distilled water. γ-Al_2O_3 powder was then dispersed in distilled water. The γ-Al_2O_3 slurry was added to the barium nitrate solution and kept for 30 min under continuous stirring. The pH value was adjusted to 11 by ammonia addition and kept for 15 min under continuous stirring. The BaO/Al_2O_3 powder was freeze dried and finally calcined in air at 550°C for 2 h. The Pt/Al_2O_3 and $Pt/BaO/Al_2O_3$ catalysts were prepared by dispersing the Al_2O_3 or BaO/Al_2O_3 powder in distilled water and adjusting the pH value to 11 by ammonia addition. Tetraammineplatinum(II)chloride was dissolved in distilled water. The solution was added to the slurry, which was then kept under continuous stirring for 1 h. The powder was freeze dried and finally calcined in air at 550°C for 2 h.

2.2. Infrared spectroscopy

The FTIR experiments were performed with thin discs with 18 mm in diameter. The discs were prepared by pressing 35 mg catalyst powder in a manual hydraulic press. A disc was placed between the two halves of a folded tungsten grid and fixed in the centre of a reaction chamber with CaF_2 windows. The reaction chamber was centred in the focal point of the IR beam in the sample compartment of a Perkin–Elmer 1700 FTIR spectrometer. The temperature was measured with a chromel–alumel thermocouple, in contact with the grid, and controlled via the voltage applied over the grid. All spectra were measured with 4 cm^{-1} resolution using a liquid nitrogen cooled MCT detector. The gas flow was parallel to the catalyst disc. The gases (supplied by AGA) had the following purity classes: N_2 (plus), O_2 (plus), H_2 (plus), 1% NO in N_2 (standard) and 1% NO_2 in N_2 (standard).

The fresh catalysts were initially reduced in 600 ppm H_2 in N_2 (total flow rate of 500 ml/min) at 450°C for 30 min. The samples were then stabilised in a sequence with 5% O_2 and 500 ppm NO in N_2 for 5 min, followed by 600 ppm H_2 in N_2 for 5 min (total flow rate 500 ml/min). This sequence was repeated six times.

A separate reference spectrum for each experiment (i.e. for each sample and temperature) was taken in

N_2 prior to introduction of nitric oxide. Storage took place during 10 min followed by regeneration during 10 min. In the storage phase the sample was exposed to 1000 ppm of either NO or NO_2 and 5% O_2 in N_2 and in the regeneration phase pure N_2 was used. Spectra were taken after 0.5, 1, 2, 4, and 8 min both during storage and in the regeneration phase. Absorbance spectra were calculated from these spectra and the reference. During the experiments 10 scans were averaged both for the reference and for each measurement.

2.3. Curve fitting

Curve fitting was performed on several spectra simultaneously. For each absorption band the band position and the bandwidth (FWHM; full width at half maximum) were kept the same for all spectra. A mixed Gaussian and Lorentzian band shape was used, where the Gaussian fraction was fitted to a common value for all spectra. The band heights were fitted individually in each spectrum. For species yielding two bands, the band height was only fitted for one of the bands and a common ratio to the other band was used for all spectra. Presence of gas phase NO_2 was taken into account by fitting the height of an extra pair of bands. A pure Gaussian band shape was used and the position, width, and relative size of the bands were determined from a separate NO_2 experiment with no catalyst disc in the reaction chamber.

Spectra of NO_x stored on Al_2O_3 and Pt/Al_2O_3 were fitted first. The initial curve fitting was performed with 40 spectra selected in order to capture different distributions of the surface species. First fitting of all bands was performed with 20 spectra with major contributions from surface nitrites and 20 spectra with major contributions from surface nitrates. A refined fitting of the nitrate bands was then performed with 40 spectra with major contributions from surface nitrates, followed by a refined fitting of the nitrite bands with 40 spectra with major contributions from surface nitrites. The curve fitting started with a spectral model consisting of only those bands that could clearly be distinguished in the spectra. Residual analysis was then used to stepwise improve the model by adding more bands. The final model contained six pairs of bands for surface nitrates, three pairs of bands for high coverage and three pairs of bands for low coverage. When fitting this model, difficulties occurred with slow convergence and convergence at local minima. These problems were partly due to that there are 720 ways to combine the six high frequency bands with the six low frequency bands. A faster convergence at a global minimum was obtained by applying constraints based on assumed physical relationships. It was assumed that the ratio for the height and width between the high and low frequency band was the same at high and low coverage, and that the shift in wave number was equal for the high and low frequency band. Curve fitting was performed once with these constraints and then repeated with the constraints successively relaxed, first the height ratio, then the wave number shift and finally without any constraints. The Gaussian fraction was fitted to a common value for all bands on Al_2O_3, since individual values for each band resulted in large confidence intervals.

When an adequate spectral model had been obtained for Al_2O_3, this model was extended with bands for nitrites and nitrates both on BaO and on Al_2O_3 close to BaO. The curve fitting was first performed with 30 spectra selected in order to capture different distributions of all the surface species associated with BaO. Refined fittings were then successively performed with 30 spectra with significant contributions from nitrates on BaO, from nitrates on Al_2O_3 close to BaO, and finally from nitrites on BaO and on Al_2O_3 close to BaO. The Gaussian fraction was fitted to a common value for all bands on BaO and on Al_2O_3 close to BaO.

3. Results and discussion

3.1. General features

In Fig. 1a spectra for Al_2O_3 after 8 min in 5% O_2 and 1000 ppm NO_2 at temperatures from 100 to 400°C are shown. Overlapping bands assigned to monodentate, bidentate and bridged nitrates [12–15] are observed around 1600 and 1250 cm^{-1}. The centre of the overlapping bands are shifted towards higher wave numbers as the temperature is decreased. When analogue experiments are performed with Pt/Al_2O_3 (not shown) similar results are obtained, but the heights of the bands are somewhat smaller. In Fig. 1b spectra for Al_2O_3 after 8 min in 5% O_2 and 1000 ppm NO at temperatures from 100 to 400°C are shown. A narrow band around 1230 cm^{-1} is observed. This

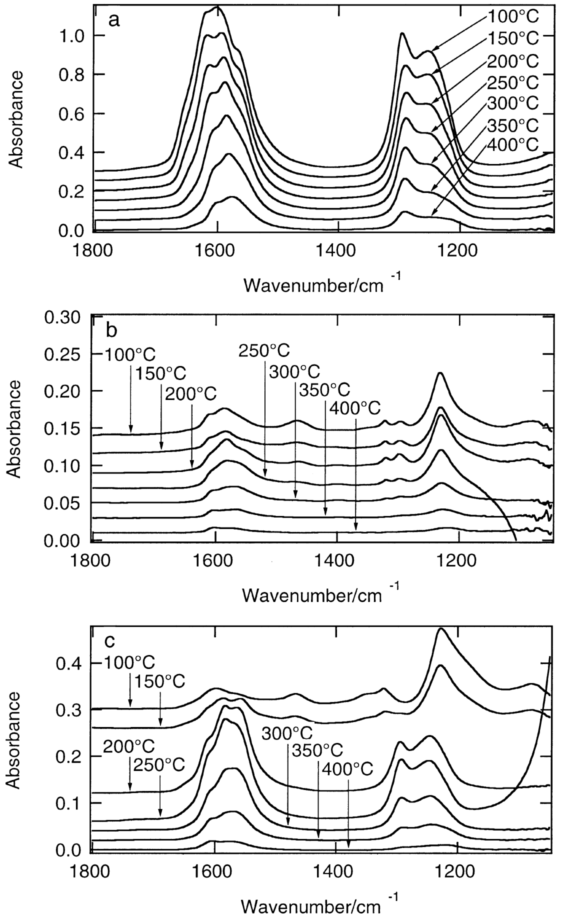

Fig. 1. FTIR spectra for: (a) Al_2O_3 exposed to 5% O_2 and 1000 ppm NO_2, (b) Al_2O_3 exposed to 5% O_2 and 1000 ppm NO, (c) Pt/Al_2O_3 exposed to 5% O_2 and 1000 ppm NO. The exposure was for 8 min at different temperatures.

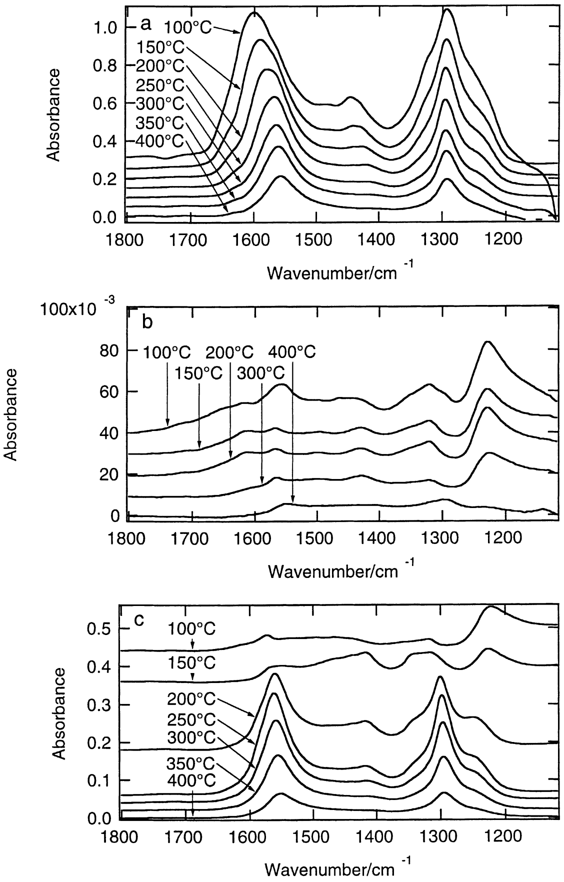

Fig. 2. FTIR spectra for: (a) BaO/Al_2O_3 exposed to 5% O_2 and 1000 ppm NO_2, (b) BaO/Al_2O_3 exposed to 5% O_2 and 1000 ppm NO, (c) Pt/BaO/Al_2O_3 exposed to 5% O_2 and 1000 ppm NO. The exposure was for 8 min at different temperatures.

band appears together with a smaller band around 1320 cm^{-1} and is assigned to bridged nitrite [12–15]. Bands around 1470 and 1080 cm^{-1} assigned to linear nitrite [12,14,15] and around 1350 cm^{-1} assigned to NO^- (hyponitrite) [15] are observed at lower temperatures. Nitrate bands are observed at all temperatures. The sizes of all bands are markedly smaller than after exposure to NO_2. In Fig. 1c the spectra of Pt/Al_2O_3 after 8 min exposure to 5% O_2 and 1000 ppm NO at temperatures from 100 to 400°C are shown. At 100 and 150°C linear nitrite, bridged nitrite and hyponitrite are observed together with small amounts of nitrates. From 200 to 400°C mainly nitrates are observed.

In Fig. 2a the spectra for BaO/Al_2O_3 after 8 min in 5% O_2 and 1000 ppm NO_2 at temperatures from 100 to 400°C are shown. Nitrate bands are observed around 1600 and 1290 cm^{-1}. As in the experiment with Al_2O_3 exposed to NO_2 and O_2, the centre of the overlapping bands are shifted towards higher wave numbers as the temperature is decreased, but the bands are narrower compared to the Al_2O_3 case. Overlapping bands are also observed around 1430 cm^{-1}. These are assigned to linear and monodentate nitrite on BaO [15]. When analogue experiments are performed with Pt/BaO/Al_2O_3 (not shown) similar results are obtained, but the nitrate bands are somewhat smaller and narrower. In Fig. 2b the spectra for

Table 1
Fitted bands for species on Al_2O_3: assignments and parameters with 95% confidence intervals[a]

Species	Structure	Remark	Position/cm^{-1}	FWHM/cm^{-1}	Height ratio
Nitrogen dioxide	NO_2 (g)		1630.4 ± 0.4	7.9 ± 0.3	1.30 ± 0.08
			1599.5 ± 0.6	11.9 ± 0.3	
Bridged nitrate	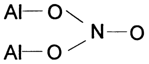	High coverage	1629.5 ± 1.3	22.9 ± 1.1	1.52 ± 0.05
			1265.7 ± 2.9	36.1 ± 2.7	
		Low coverage	1605.6 ± 0.6	7.6 ± 0.2	1.68 ± 0.20
			1210.8 ± 1.0	15.4 ± 0.6	
Bidentate nitrate	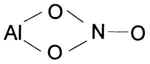	High coverage	1611.6 ± 1.4	11.7 ± 0.5	1.28 ± 0.18
			1292.5 ± 0.7	14.8 ± 0.8	
		Low coverage	1570.9 ± 1.1	29.6 ± 0.4	1.79 ± 0.08
			1249.2 ± 1.2	27.9 ± 1.4	
Monodentate nitrate	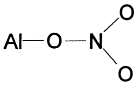	High coverage	1588.0 ± 1.5	9.6 ± 0.3	1.44 ± 0.18
			1296.9 ± 0.6	7.1 ± 0.4	
		Low coverage	1574.7 ± 1.6	22.4 ± 0.6	0.95 ± 0.08
			1291.7 ± 0.4	14.1 ± 0.5	
Bridged nitrite	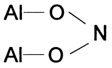		1319.8 ± 0.6	8.4 ± 0.5	0.20 ± 0.01
			1230.7 ± 0.2	13.4 ± 0.2	
N-coordinated nitrite	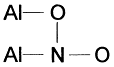		1522.5 ± 4.3	56.9 ± 3.4	1.36 ± 0.11
			1127.7 ± 2.8	27.9 ± 3.4	
Linear nitrite	Al—O—N—O		1464.4 ± 0.7	19.4 ± 0.9	0.57 ± 0.02
			1083.8 ± 0.7	25.3 ± 0.7	
Bulk nitrate	$Al^+NO_3^-$		1397.0 ± 2.2	21.3 ± 2.6	
Hyponitrite	Al^+NO^-		1343.3 ± 1.5	26.1 ± 1.8	
Superoxide	$Al^+O_2^-$		1196.2 ± 1.1	35.1 ± 0.7	

[a] The common value for band shape was fitted to 0.710 ± 0.012 Gaussian fraction.

BaO/Al_2O_3 after 8 min in 5% O_2 and 1000 ppm NO at temperatures from 100 to 400°C are shown. Overlapping bands of small amplitude are observed in the 1200 to 1600 cm^{-1} range. The most apparent band is observed at 1230 cm^{-1}, and is associated with bridged nitrite on Al_2O_3 [12–15]. In Fig. 2c the spectra for $Pt/BaO/Al_2O_3$ after 8 min in 5% O_2 and 1000 ppm NO at temperatures from 100 to 400°C are shown. At 100 and 150°C the spectra consists mainly of overlapping bands of small amplitude and one distinguishable band at 1230 cm^{-1} associated with bridged nitrite. From 200 to 400°C two sharp nitrate bands around 1290 and 1560 cm^{-1} are observed. Bands are also observed around 1430 cm^{-1}.

3.2. Analysis of fitted spectra of species on Al_2O_3

A spectral model consisting of total 21 bands was used to fit the spectra of NO_x adsorbed on Al_2O_3 and Pt/Al_2O_3. In Table 1 all parameters used in the model can be found together with 95% confidence intervals. Six pair of bands was required for surface nitrates, two pair each (one for low coverage and one for high coverage) for monodentate, bidentate and bridged nitrate. Three pair of bands was used for linear, bridged and N-coordinated nitrite [15]. A single band was used for surface species assigned to NO^-, O_2^- and bulk nitrate. In Fig. 3 experimental and corresponding fitted spectra from three representative experiments are shown. In Fig. 3a the experimental and the fitted spectra of Al_2O_3 after 0.5, 1, 2, 4 and 8 min in 5% O_2 and 1000 ppm NO at 200°C are shown. The spectra have a large contribution from nitrites, and the spectral model is able to accurately reproduce this. In Fig. 3b the experimental and the fitted spectra of Al_2O_3 after 0.5, 1, 2, 4 and 8 min in 5% O_2 and 1000 ppm NO_2 at 200°C are shown. The spectra have a large contribution from nitrates, and the spectral model is able to accurately reproduce this. At high coverages of nitrates (after 8 min exposure) there is however, a lack of fit around 1610 cm^{-1}. In Fig. 3c the experimental and the fitted spectra of Pt/Al_2O_3 after 0.5, 1, 2, 4 and 8 min in 5% O_2 and 1000 ppm NO at 200°C are shown. These spectra have a large contribution from both nitrates and nitrites and the fit is not perfect around 1580, 1290 and 1240 cm^{-1} for 2, 4 and 8 min exposures.

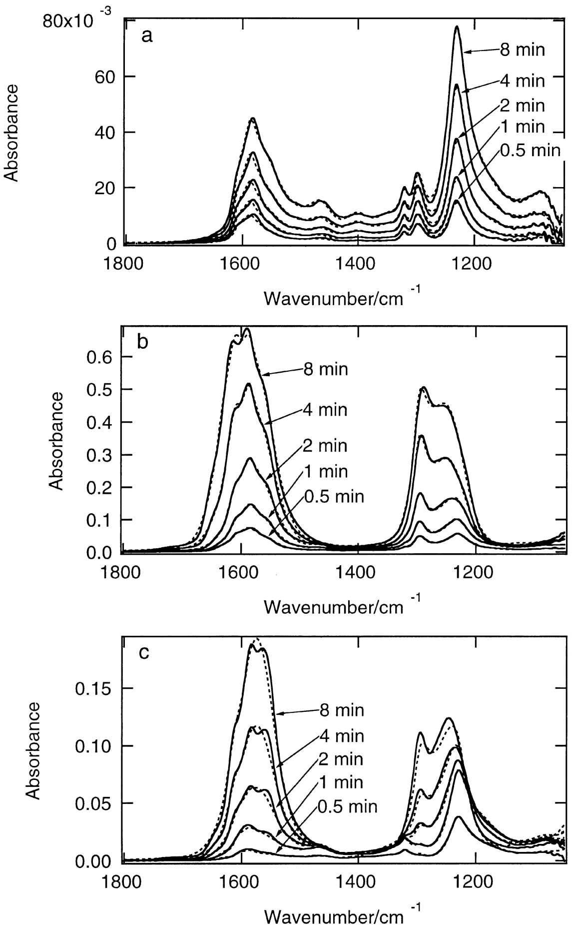

Fig. 3. Experimental (solid) and fitted (dotted) spectra at different times of exposure: (a) for Al_2O_3 in 5% O_2 and 1000 ppm NO at 200°C, (b) for Al_2O_3 in 5% O_2 and 1000 ppm NO_2 at 200°C, (c) for Pt/Al_2O_3 in 5% O_2 and 1000 ppm NO at 200°C.

In Table 2 the band centre and the splitting of the nitrate bands are listed. When the coverage is increased the nitrate bands shift to higher wave numbers. The increase in coverage also causes a change in the splitting of the bands. It is known that nitrate bands are sensitive to changes in the ionic-covalent properties of the bonding to the surface [15]. Both the position of the band centre and the splitting are affected. For organic nitrates, which can be considered as covalently bonded, the band centre is usually around 1460 cm^{-1} [16], while for inorganic nitrate salts, which can be considered as ionic, there is a degenerate band around 1380 cm^{-1} [15,16]. A covalently bonded nitrate group has a smaller electron density than an ionic nitrate group, so a shift of the band centre can be interpreted in terms of electron donation and withdrawal. The band splitting increases with increasing covalent bonding and also with increased number of bonds. For surface bonded nitrates on Al_2O_3 (Fig. 3) the band splitting is largest for bridged nitrate, bidentate nitrate has a smaller band splitting and monodentate nitrate has the smallest band splitting [15].

The shift is 40, 42 and 9 cm^{-1} for bridged, bidentate and monodentate nitrate, respectively. In view of the discussion above, a possible explanation for this is that electrons are drawn from the nitrate groups and to a higher extent for bridged and bidentate nitrate. For bridged and bidentate nitrate the splitting decrease by 31 and 3 cm^{-1}, respectively, while for

Table 2
Band centre position and splitting of the nitrate bands on Al_2O_3

Nitrate type	Coverage	ν/cm^{-1}	ν/cm^{-1}
Bridged	High	1448	364
	Low	1408	395
Bidentate	High	1452	319
	Low	1410	322
Monodentate	High	1442	291
	Low	1433	283

monodentate it increases by 8 cm^{-1}. For monodentate nitrate both the shift and the change in splitting implies a somewhat more covalent bonding with increased coverage. For bridged and bidentate nitrate the shift imply a more covalent bonding. However, the splitting decrease, and this we tentatively attribute to a decrease in bond order rather than to a less covalent bonding. Both the high and low coverage bands can be observed simultaneously. This applies specially for bidentate nitrate, for which the low coverage band can be observed even at relatively high coverages.

The band at 1397 cm^{-1} assigned as bulk nitrate [15,16] is small in all experiments and the band area can only be significantly determined in the experiments where Al_2O_3 is exposed to NO and O_2 at 200 to 300°C. During regeneration at these temperatures the size of the band decreases.

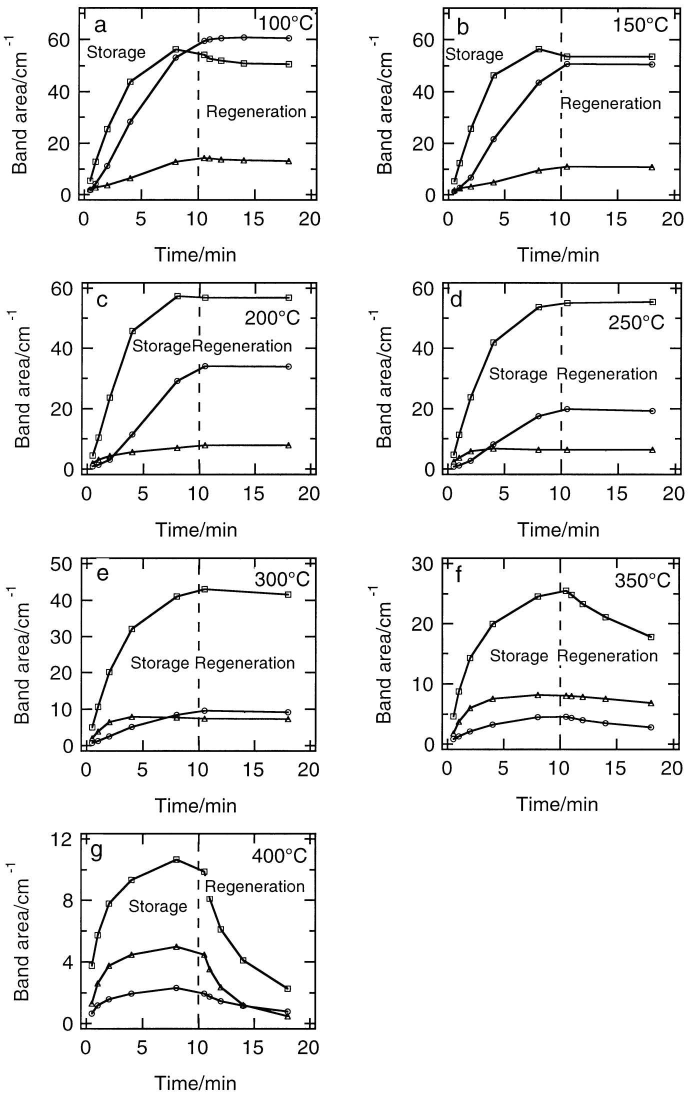

Fig. 4. The evolution in time of different types of surface nitrates for Al_2O_3 during storage in 1000 ppm NO_2 and 5% O_2 and regeneration at different temperatures (a–g): bridged nitrate (circles), bidentate nitrate (squares), monodentate nitrate (triangles).

The band at 1522 cm^{-1} appears together with overlapping nitrate bands and is difficult to distinguish. It is assigned as N-coordinated nitrite [15] that also has a second band at 1128 cm^{-1}.

The superoxide ion is observed mainly at low temperatures (100 and 150°C) on both Al_2O_3 and Pt/Al_2O_3. It is present initially in the storage period when storage is performed with NO_2 and O_2, and during the entire experiment when storage is performed with NO and O_2. It may be formed from molecular adsorption of O_2 on coordinatively unsaturated Al atoms [15] that appear during the NO or NO_2 exposure.

The relative distribution between the different nitrate species change with temperature. In Fig. 4a–g the band areas for different nitrate species are plotted versus time when Al_2O_3 is exposed to NO_2 and O_2 at temperatures from 100 to 400°C. At 100°C bridged nitrate has the largest band area. When the temperature is increased a larger contribution comes from bidentate and monodentate nitrate and at 350°C bridged nitrate has the smallest band area. At low temperatures there is a change in the band area between the last measurement in the storage period at 8 min and the first measurement in the regeneration period at 10.5 min. After this change the relative distribution between the different nitrate species remain the same. This indicates that equilibrium is established between the different nitrate species during the first 30 s after the storage has been interrupted. By calculating the equilibrium constant from the band area at several temperatures the enthalpy change for the transition between the different nitrate species can be determined. The entropy change can be determined at the same time, but attached with an error equal to the molar gas constant times the natural logarithm of the ratio between the molar absorption coefficients for the different nitrate species. However, as the molar absorption coefficients for the different nitrate species can be expected to be close to each other, this error can be expected to be small. The obtained enthalpy changes for transition from monodentate to bridged nitrate and from monodentate to bidentate nitrate are -7.7 and 7.4 kJ/mol, respectively. The corresponding entropy changes for transition from monodentate to bridged nitrate and from monodentate to bidentate nitrate are -7.1 and 30.2 J/mol K, respectively. These values indicate that the strength of the bond to the surface increase in the order bidentate $<$ monodentate $<$ bridged nitrate. The mobility of the nitrate species increases in the opposite order, with bidentate nitrate being the most mobile nitrate species. This also agrees with the adsorption and desorption behaviour of the nitrate species (Fig. 4f and g). At 350°C bidentate nitrate desorbs faster than monodentate and bridged nitrate and at 400°C both bidentate and monodentate nitrate desorbs faster than bridged nitrate. At all temperatures bidentate nitrate has a first order response to the NO_2 plus O_2 exposure, indicating that it is a primary product, while bridged nitrate has a second order response at temperatures up to 250°C, indicating that it is a secondary product. At 250 and 300°C monodentate nitrate has reached steady state after 4 min while bidentate and bridged nitrate have not reached steady state after 8 min. This behaviour is in accordance with monodentate nitrate being an intermediate product.

In Fig. 3c it can be noticed that when Pt/Al_2O_3 is exposed to NO and O_2 at 200°C the band associated with bridged nitrite at 1230 cm^{-1} is the most distinct band during the first 2 min. After 4 min the nitrate bands are larger. In Fig. 5b the total band areas for

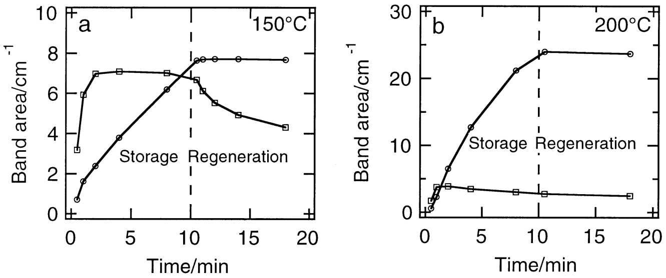

Fig. 5. The evolution in time of nitrates (circles) and nitrites (squares) for Pt/Al_2O_3 during storage in 1000 ppm NO and 5% O_2 and regeneration: (a) $T = 150°C$, (b) $T = 200°C$.

nitrites and nitrates are plotted versus time. The coverage of nitrites reach steady state after 1 min and after 2 min it decreases slowly. The nitrate coverage increases during the entire storage period, with a small decrease in the formation rate with time. When the same experiment is performed at 150°C (Fig. 5a) it can be observed that the nitrite coverage reach steady state after 2 min and then remains at steady state during the entire storage period. The nitrate coverage increases linearly after 1 min until the end of the storage period. This suggests that the formation of nitrates proceed via the formation of nitrites. During the regeneration period the nitrates remain at the same coverage while the coverage of nitrites decreases.

In Fig. 6 the band areas for the different nitrate species are plotted versus time for Pt/Al_2O_3 exposed to NO_2 and O_2 at (a) 250°C, (b) 300°C and (c) to NO and O_2 at 300°C. At 250°C the nitrates are stable on Al_2O_3 (Fig. 4d), while the nitrate coverage on Pt/Al_2O_3 slowly decreases during the regeneration period (Fig. 6a). Bridged nitrate decreases more rapidly than bidentate and monodentate nitrate. The total amount of nitrates is smaller on Pt/Al_2O_3 and the relative amount of bridged nitrate is also smaller. At 300°C there is a slow decrease in the nitrate coverage on Al_2O_3 (Fig. 4e), while on Pt/Al_2O_3 the decrease is fast (Fig. 6b). At this temperature the coverage of bidentate and bridged nitrate decreases faster than the coverage of monodentate nitrate. These observations indicate that it is mainly the coverage of bridged nitrate that is influenced by the presence of Pt. This influence is probably indirect via the NO_2 decomposition reaction on Pt. When the storage is performed with NO and O_2 at 300°C on Pt/Al_2O_3 (Fig. 6c) the coverage of bridged nitrate reach maximum after 4 min and then slowly decreases. The relative amount of bridged nitrate is low during the entire experiment and the total amount of nitrates is less than half of the amount when storage is performed with NO_2 and O_2. This observation indicates that the coverage of bridged nitrate is suppressed by the presence of NO in the gas.

3.3. Analysis of fitted spectra of species on BaO/Al_2O_3

Eleven additional bands were needed to fit the spectra of NO_x adsorbed on BaO/Al_2O_3 and Pt/BaO/Al_2O_3. In Table 3 all parameters used in the

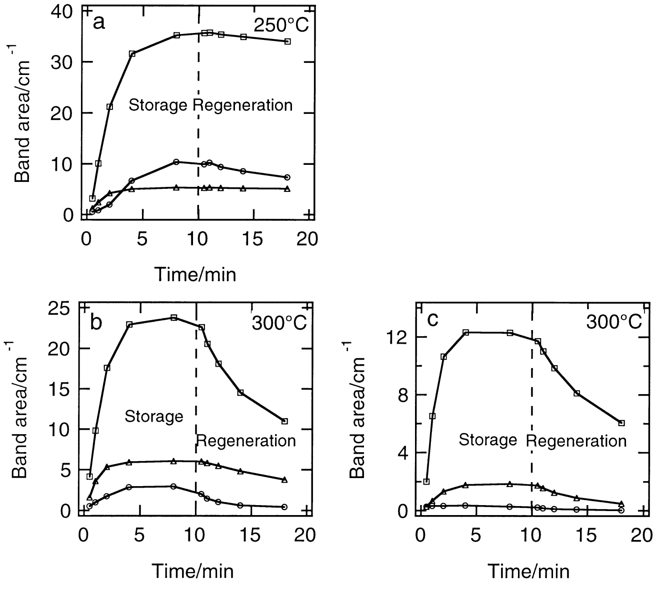

Fig. 6. The evolution in time of different types of surface nitrates for Pt/Al_2O_3: (a) in 5% O_2 and 1000 ppm NO_2 at 250°C, (b) in 5% O_2 and 1000 ppm NO_2 at 300°C, (c) in 5% O_2 and 1000 ppm NO at 300°C; bridged nitrate (circles), bidentate nitrate (squares), monodentate nitrate (triangles).

Table 3
Fitted bands for species associated with BaO: assignments and parameters with 95% confidence intervals[a]

Species	Structure	Position/cm^{-1}	FWHM/cm^{-1}	Height ratio
Monodentate nitrate on Ba	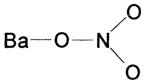	1542.0 ± 0.6	20.3 ± 0.3	0.74 ± 0.02
		1291.4 ± 0.3	20.5 ± 0.9	
Bridged nitrate on Al close to Ba	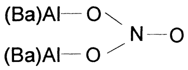	1572.9 ± 1.7	7.4 ± 0.3	1.46 ± 0.33
		1214.0 ± 1.8	11.4 ± 0.5	
Bidentate nitrate on Al close to Ba	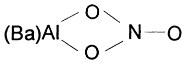	1559.5 ± 0.8	13.1 ± 0.2	1.90 ± 0.08
		1245.4 ± 1.8	14.5 ± 1.4	
Monodentate nitrite on Ba	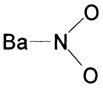	1411.5 ± 2.0	17.1 ± 1.9	2.23 ± 0.35
		1307.6 ± 1.5	7.9 ± 0.9	
Linear nitrite on Ba	Ba—O—N—O	1434.2 ± 1.3	18.7 ± 1.2	
N-coordinated nitrite on Al close to Ba	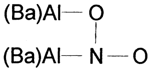	1491.4 ± 2.6	46.0 ± 4.7	
Hyponitrite on Ba	Ba$^+$NO$^-$	1316.4 ± 4.4	32.3 ± 0.8	

[a] The common value for band shape was fitted to 0.863 ± 0.022 Gaussian fraction.

model can be found together with 95% confidence intervals. A pair of bands was used for surface nitrates on BaO and two additional pairs of bands for nitrates were also required. These are below assigned as bidentate and bridged nitrates on Al_2O_3 close to BaO. Thus, in order to fit the data we assume that a special type of binding site is formed at the interface between BaO and Al_2O_3. Bands for monodentate nitrate on Al_2O_3 close to BaO could not be fitted with significance. One pair of bands was used for monodentate nitrite on BaO (nitro group), and single bands were used for linear nitrite and hyponitrite on BaO and N-coordinated nitrite on Al_2O_3 close to BaO. The low frequency bands of linear nitrite on BaO and N-coordinated nitrite on Al_2O_3 close to BaO were below the cut-off frequency for the BaO/Al_2O_3 system and could not be fitted. No band for barium nitrate bulk could be fitted with significance. In Fig. 7 experimental and the corresponding fitted spectra from three representative experiments are shown. In Fig. 7a the experimental and the fitted spectra of Pt/BaO/Al_2O_3 after 0.5, 1, 2, 4 and 8 min in 5% O_2 and 1000 ppm NO at 150°C are shown. The spectra have a large contribution from nitrites and also some contribution from nitrates, and the spectral model is able to reproduce most of the features accurately. It is however, obvious that the fit is poor around 1350 cm^{-1}. In Fig. 7b the experimental and the fitted spectra of BaO/Al_2O_3 after 0.5, 1, 2, 4 and 8 min in 5% O_2 and 1000 ppm NO_2 at 200°C are shown. The spectra have a large contribution from nitrates, and the spectral model is able to accurately reproduce this. In Fig. 7c the experimental and the fitted spectra of Pt/BaO/Al_2O_3 after 0.5, 1, 2, 4 and 8 min in 5% O_2 and 1000 ppm NO at 200°C are shown. These spectra have a large contribution from both nitrates and nitrites and the spectral model is able to reproduce most of the features accurately. There is a slight lack of fit around 1260 cm^{-1} for 4 and 8 min exposures.

In Table 4 the band centre and the splitting of the nitrate bands associated with BaO are listed. The splitting values for the first two species are similar to those of bridged and bidentate nitrate at high coverage on Al_2O_3. We assign these species as bridged and

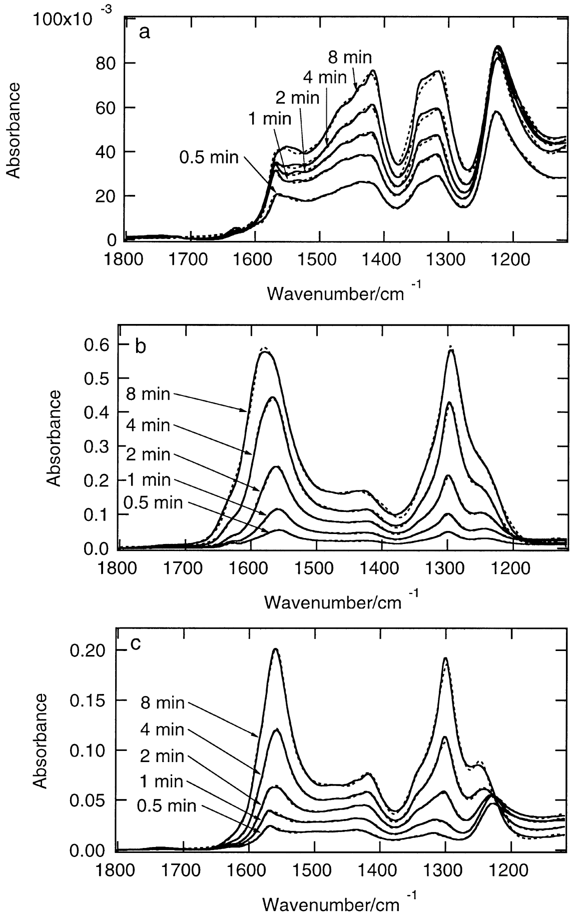

Fig. 7. Experimental (solid) and fitted (dotted) spectra at different times of exposure: (a) for Pt/BaO/Al_2O_3 in 5% O_2 and 1000 ppm NO at 150°C, (b) for BaO/Al_2O_3 in 5% O_2 and 1000 ppm NO_2 at 200°C, (c) for Pt/BaO/Al_2O_3 in 5% O_2 and 1000 ppm NO at 200°C.

bidentate nitrate on Al_2O_3 close to BaO. The positions of the band centre are however, at frequencies lower than those of bridged and bidentate nitrate at low coverage on Al_2O_3. A possible explanation for this is donation of electrons from Ba, which may as discussed above cause a shift towards higher binding energies for nitrates on alumina. The band centre for monodentate nitrate on BaO is at a lower frequency than for monodentate nitrate on Al_2O_3 and the band splitting is also smaller. This may be related to the higher degree of ionic bonding for monodentate nitrate that can be expected for Ba compared with Al.

Table 4
Band centre position and splitting of the nitrate bands associated with BaO

Nitrate type	ν/cm^{-1}	ν/cm^{-1}
Bridged nitrate on Al close to Ba	1394	359
Bidentate nitrate on Al close to Ba	1403	315
Monodentate nitrate on Ba	1417	252

A separate band for $Ba(NO_3)_2$ could not be fitted with significance for the BaO containing samples. The reason for this may be that the size and the position of that band is very similar to those for bulk nitrate on Al_2O_3. An increase of the band area for bulk nitrate on Al_2O_3 was observed when compared to the system without BaO. This increase could indicate that some $Ba(NO_3)_2$ is formed. However, the band area is still small compared to the band area for surface nitrates. The reason that no significant formation of $Ba(NO_3)_2$ is observed is probably the relatively low NO_x exposures (still relatively high in relation to lean-burn engine exhaust). Mahzoul et al. [17] observe bulk nitrate only after an exposure time of 20 min with similar concentrations. Coronado and Anderson [6] who observed NO_3 anions, had similar conditions as in this work but a different support (SiO_2) with a smaller surface area.

In Fig. 8a–g the total band areas for the different nitrate species are plotted versus time when BaO/Al_2O_3 is exposed to NO_2 and O_2 at temperatures from 100 to 400°C. At 100 and 150°C nitrates are formed almost exclusively on Al_2O_3. At 200°C a small amount of nitrate on BaO is formed. The relative amount of nitrate on BaO increases with temperature, and at 350°C the band area for nitrate on BaO is larger than for the other nitrate types. The relative amount of bridged nitrate on Al_2O_3 is smaller at all temperatures compared to when the Al_2O_3 sample is exposed to NO_2 and O_2. The relative amount of bridged nitrate on Al_2O_3 close to BaO is small at all temperatures compared to other types of nitrates. At temperatures from 200°C and higher the band areas associated with nitrate on BaO and bidentate nitrate on Al_2O_3 close to BaO increase more rapidly than the band areas associated with bridged, bidentate and monodentate nitrate on Al_2O_3. This suggests that nitrates are formed on Al_2O_3 and then move to BaO. At temperatures up to 300°C the band area for bidentate nitrate on Al_2O_3 close to BaO goes through a maximum. The band area for nitrate on BaO also goes through a maximum at temperatures up to 250°C.

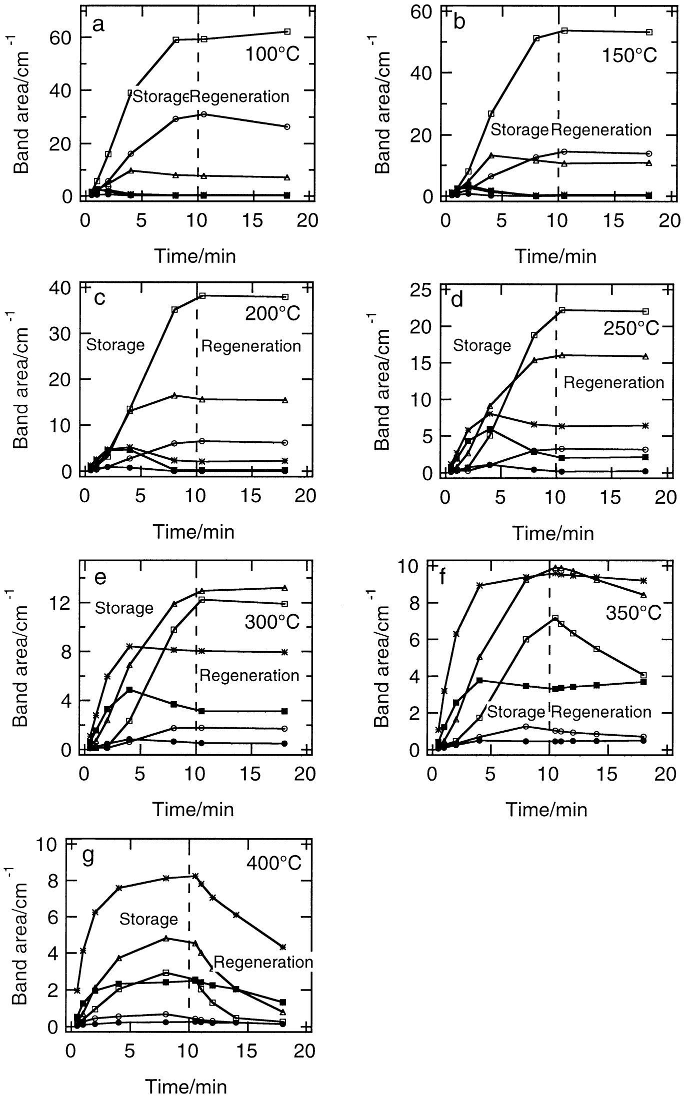

Fig. 8. The evolution in time of different types of surface nitrates for BaO/Al_2O_3 during storage in 1000 ppm NO_2 and 5% O_2 and regeneration at different temperatures (a–g): bridged nitrate on Al_2O_3 (open circles), bidentate nitrate on Al_2O_3 (open squares), monodentate nitrate on Al_2O_3 (triangles), monodentate nitrate on BaO (stars), bridged nitrate on Al_2O_3 close to BaO (filled circles), bidentate nitrate on Al_2O_3 close to BaO (filled squares).

The reasons for this is discussed below. At 350°C the coverage of nitrates on BaO decreases slowly during the regeneration period while the coverage of nitrates on Al_2O_3 decreases more rapidly. The coverage of nitrates on Al_2O_3 close to BaO increases slightly. At 400°C the coverage of all nitrates decreases during the regeneration period. The coverage of nitrates on BaO decreases more rapidly than the coverage of nitrates on Al_2O_3 close to BaO, and the coverage of nitrates on Al_2O_3 decreases fastest of all nitrate types.

In Fig. 9a–d the total band areas for N-coordinated nitrite on Al_2O_3 close to BaO, as well as hyponitrite, monodentate and linear nitrite on BaO are plotted versus time when the BaO/Al_2O_3 sample is exposed to

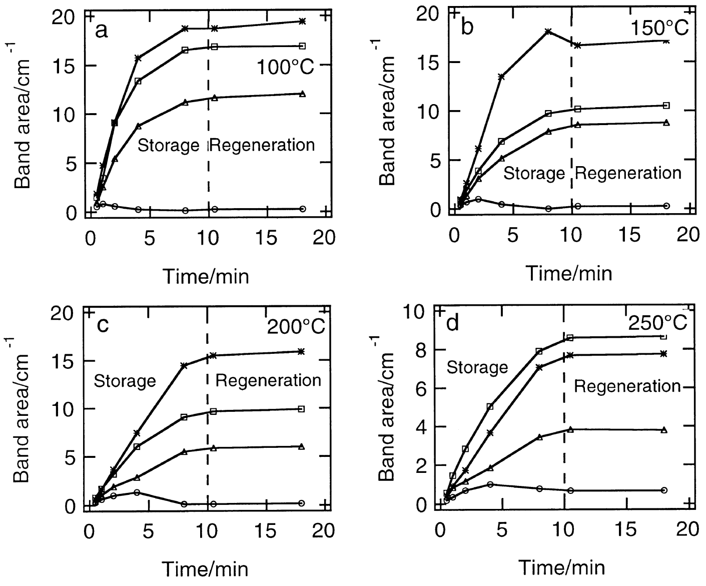

Fig. 9. The evolution in time of different surface species for BaO/Al_2O_3 during storage in 1000 ppm NO_2 and 5% O_2 and regeneration at different temperatures (a–d): N-coordinated nitrite on Al_2O_3 close to BaO (squares), hyponitrite (stars), linear nitrite on BaO (triangles), monodentate nitrite on BaO (circles).

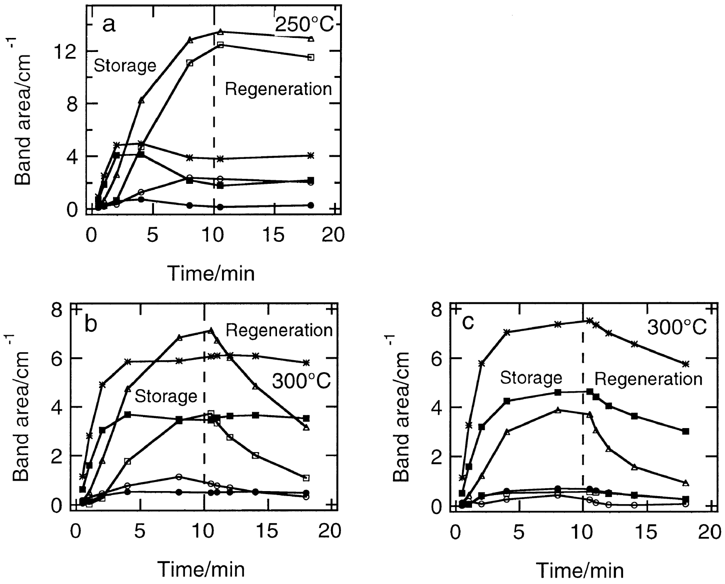

Fig. 10. The evolution in time of different types of surface nitrates for Pt/BaO/Al_2O_3: (a) in 5% O_2 and 1000 ppm NO_2 at 250°C, (b) in 5% O_2 and 1000 ppm NO_2 at 300°C, (c) in 5% O_2 and 1000 ppm NO at 300°C; bridged nitrate on Al_2O_3 (open circles), bidentate nitrate on Al_2O_3 (open squares), monodentate nitrate on Al_2O_3 (triangles), monodentate nitrate on BaO (stars), bridged nitrate on Al_2O_3 close to BaO (filled circles), bidentate nitrate on Al_2O_3 close to BaO (filled squares).

NO_2 and O_2 at temperatures from 100 to 250°C. It can be noticed that the amount of N-coordinated nitrite on Al_2O_3 close to BaO as well as the linear nitrite and hyponitrite on BaO all increase during the entire storage period at all four temperatures. During the regeneration period the amount of these species remain constant. The coverage of monodentate nitrite seems to be slightly correlated with the coverage of nitrate on BaO. If we assume that there is an equilibrium reaction where hyponitrite and nitrate yield two surface nitrites and that this reaction proceeds on both the BaO and the Al_2O_3 surface we may explain the observations that bidentate nitrate on Al_2O_3 close to BaO and nitrate on BaO goes through a maximum at 100–250°C. For this explanation to be feasible, the coverage of hyponitrite must increase rapidly compared with the nitrite coverage. For hyponitrite and nitrites on BaO this can also be observed after the initial storage at 100 to 250°C.

In Fig. 10 the total band areas for the different nitrate species are plotted versus time when $Pt/BaO/Al_2O_3$ is exposed to NO_2 and O_2 at (a) 250°C, (b) 300°C and (c) to NO and O_2 at 300°C. On BaO/Al_2O_3 all nitrates are practically stable at 250 and 300°C (Fig. 8d and e). On $Pt/BaO/Al_2O_3$ the coverage of nitrates on Al_2O_3 slowly decreases during the regeneration period at 250°C (Fig. 10a), while the coverage of nitrates on BaO and on Al_2O_3 close to BaO slowly increases. At 300°C the coverage of nitrates on Al_2O_3 decreases more rapidly while the coverage of nitrates on BaO and on Al_2O_3 close to BaO goes through a maximum (Fig. 10b). These observations indicate that the presence of Pt mainly influences the stability of the nitrates on Al_2O_3. When $Pt/BaO/Al_2O_3$ is exposed to NO and O_2 at 300°C (Fig. 10c) the amount of bridged nitrate is markedly smaller than after exposures to NO_2 and O_2. This observation is in accordance with the discussion above that NO suppresses the coverage of bridged nitrate.

4. Summary and conclusions

FTIR spectroscopy has been used to study samples of Al_2O_3, Pt/Al_2O_3, BaO/Al_2O_3 and $Pt/BaO/Al_2O_3$ under exposure to either NO_2 and O_2 or NO and O_2, between 100 and 400°C. The resulting spectra are fitted to various species, mainly nitrites and nitrates, formed on Al_2O_3 and BaO. The exposure of NO_2 and O_2 on the Al_2O_3 sample results in the formation of monodentate, bridged and bidentate nitrates. The relative abundance of these nitrate species change with temperature. The obtained enthalpy changes for transition from monodentate to bridged nitrate and from monodentate to bidentate nitrate are -7.7 and 7.4 kJ/mol, respectively. And the corresponding entropy changes are -7.1 and 30.2 J/mol K, respectively. For NO and O_2, lower concentrations of nitrates are detected as well as both linear and bridged nitrites. When Pt is present in the catalyst, NO is oxidised to NO_2 at temperatures above 150°C resulting in the formation of large amounts of nitrates. It seems as if the formation of nitrites proceed the formation of nitrates.

For the samples with both BaO and Al_2O_3, similar features on Al_2O_3 as discussed above are seen. On BaO mainly nitrites and hyponitrites are observed when exposed to $NO + O_2$ below 200°C. When exposed to $NO_2 + O_2$, nitrates on BaO are found as well as two features attributed to bidentate and bridged nitrate on alumina at the alumina–barium oxide interface. At temperatures above 350°C surface nitrates on BaO is the most abundant species. The data indicates that nitrate groups may move from Al_2O_3 to BaO during storage. Formation of bulk $Ba(NO_3)_2$ was not observed. Pt is found to mainly influence the stability of nitrates on alumina. Al_2O_3 is found to be important as a storage site at temperatures below 300°C.

Acknowledgements

The Competence Centre for Catalysis is financially supported by the Swedish National Energy Administration and the member companies: AB Volvo, Johnson Matthey CSD, Saab Automobile AB, Perstorp AB, MTC AB and Eka Chemicals AB. The authors wish to thank Su Lan Xu for help with the measurements and Dr. Bo Albinsson for technical assistance. Fruitful discussions with Dr. Hans Persson and Dr. Magnus Skoglundh are gratefully acknowledged.

References

[1] M. Shelef, Chem. Rev. 95 (1995) 209.
[2] N. Takahashi, H. Shinjoh, T. Iijima, T. Suzuki, K. Yamazaki, K. Yokota, H. Suzuki, N. Miyoshi, S. Matsumoto, T. Tanizawa, T. Tanaka, S. Tateishi, K. Kasahara, Catal. Today 27 (1996) 63.

[3] W. Bögner, M. Krämer, B. Krutzsch, S. Pischinger, D. Voigtländer, G. Wenninger, F. Wirbeleit, M.S. Brogan, J. Brisley, D.E. Webster, Appl. Catal. B 7 (1995) 153.

[4] E. Fridell, M. Skoglundh, B. Westerberg, S. Johansson, G. Smedler, J. Catal. 183 (1999) 196.

[5] E. Fridell, M. Skoglundh, S. Johansson, B. Westerberg, A. Törncrona, G. Smedler, Stud. Surf. Sci. Catal. 116 (1998) 537.

[6] J.M. Coronado, J.A. Anderson, J. Mol. Catal. A 138 (1999) 83.

[7] V.I. Parvulescu, P. Grange, B. Delmon, Catal. Today 46 (1998) 233.

[8] T. Okuhara, Y. Hasada, M. Misono, Catal. Today 35 (1997) 83.

[9] D.K. Captain, M.D. Amiridis, J. Catal. 184 (1999) 377.

[10] G.R. Bamwenda, A. Ogata, A. Obuchi, J. Oi, K. Mizunoand, J. Skrzypek, Appl. Catal. B 6 (1995) 311.

[11] F. Acke, L. Eriksson, B. Westerberg, M. Skoglundh, E. Fridell, S. Johansson, G. Smedler, Stud. Surf. Sci. Catal. 116 (1998) 285.

[12] W.S. Kijlstra, D.S. Brands, E.K. Poels, A. Bliek, J. Catal. 171 (1997) 208.

[13] A.L. Goodman, T.M. Miller, V.H. Grassian, J. Vac. Sci. Technol. A16 (1998) 2585.

[14] D.V. Pozdnyakov, V.N. Filimonov, Adv. Mol. Rel. Proc. 5 (1973) 55.

[15] A.A. Davydov, Infrared Spectroscopy of Adsorbed Species on the Surface of Transition Metal Oxides, Wiley, New York, 1990.

[16] N.B. Colthup, L.H. Daly, S.E. Wiberley, Introduction to Infrared and Raman Spectroscopy, Academic Press, New York, 1990.

[17] H. Mahzoul, J.F. Brilhac, P. Gilot, Appl. Catal. B 20 (1999) 47.